Modeling and Simulation Framework for Assessing Interference in Multi-Hop Wireless Ad Hoc Networks

Shinuk Woo, Jinpyo Hong, and Hwangnam Kim
School of Electrical Engineering, Korea University
Anam-Dong, Seongbuk-Gu, Seoul 136-713, Korea
[e-mail: {wsu1027, jpsps, hnkim}@korea.ac.kr]
*Corresponding author: Hwangnam Kim

Received December 16, 2008; revised January 14, 2009; accepted January 17, 2009; published February 23, 2009

Abstract

In this paper, we propose an empirical framework for modeling and emulating interference in multi-hop wireless ad-hoc networks. Wireless interference causes wide variation in the frame delivery rate at a link, and thus we cannot represent the state of the link with only two states, *connected* state and *disconnected* state, as in wired networks. We first investigate wireless interference in detail, in order to accurately calibrate the interference and identify its underlying attributes, and then we simulate the diverse occurrences and effects of interference, after incorporating the scheme into a simulation tool. Based on these observations, we devise a modeling and simulation framework with several control parameters, and perform an extensive set of simulation studies. The simulation results indicate that the proposed framework enables us to examine various attributes of wireless interferences and their effects on wireless network protocols and systems.

Keywords: Interference, SINR, frame delivery rate, IEEE 802.11, wireless LAN, modeling and simulation

This work was supported in part by the Korea Science and Engineering Foundation (KOSEF) grant funded by the Korea government (MOST) (No. R01-2007-000-20958-0), and in part by the IT R&D program of MKE/IITA [2008-F-015-01, Research on Ubiquitous Mobility Management Methods for Higher Service Availability].

DOI: 10.3837/tiis.2009.01.002

1. Introduction

In multi-hop wireless ad-hoc networks, wireless links are exposed to hostile radio environments resulting from various types of interferences, such as shadowing, reflection, refraction, scattering, diffraction, inter-symbol interference, and fading. Wireless links thus cannot permanently remain in the state where they are *connected* to neighboring nodes and capable of successful transmission, viz., ON state, or in the opposite state where they are *disconnected* from these nodes and incapable of successful transmission, viz., OFF state. In other words, each wireless link state can have any level of connection with neighboring stations between *connected* and *disconnected* states, even from time to time, which means that the links do not always successfully transmit a frame nor fail to deliver frame in a given interval. We usually represent the degree of reliability at a link by the *frame delivery rate* (FDR) of the link; the information about FDR is one of important keys in order to improve the correctness and performance of wireless ad-hoc network systems, and can be exploited to improve routing, auto-rate-fallback (ARF), topology control (TC) and any other protocol developed and deployed for wireless networks. However it is not easy to determine or estimate FDR, since we can hardly identify all the attributes that contributed to it, such as SINR (Signal to Interference Noise Ratio) and the aforementioned interferences. Also their combinations change over time.

Even though there is a sharp theoretical gap separating the *connected* and *disconnected* states in the range of the SINR values (3dB), which is only realized when there is no external environmental effect, the measured gap is much wider than 3dB in a real-world environment, i.e. the results of MIT Roofnet [1]. This observation indicates that there is an intermediate range of SINR values that incurs an intermediate FDR. Therefore we need to consider this intermediate FDR in protocols and/or systems used in wireless networks. For example, routing algorithms should not always regard the path with the least number of hops as the best path [2] since a path with shorter hops may require more transmissions to successfully deliver a frame to the destination, due to an unreliable link state, i.e. a lower FDR [3][4]. Additionally, geographic routing can also use link state information to choose the best next-hop among several candiates that are close to a destination [5]. Moreover, MAC protocols can improve their capacity if they can determine the exact reason for a frame loss, such as severe contention, interference, or network-level congestion [6]: for example, if the loss is incurred by interference, the MAC protocols do not need to increase their contention window size in order to avoid contention with neighboring stations. In fact, we have several works in the literature each of which use a measurement-based method and profiling to measure and improve the link capacity and throughput [7][8][9][10][11].

In this paper, we propose a modeling and simulation framework to investigate the characteristics of wireless interference or to regenerate the interferences for the purpose of conducting a rigorous analysis about their impact on wireless networking protocols and systems. The framework depends on accurate information about the relationship between FDR and SINR. In order to determine the relationship, we first constructed an elaborate scheme for calculating the wireless interference within one received frame, then incorporated it into the *ns-2* simulation tool, and conducted a set of simulations. In the simulation, we observed that FDR varies even for the same SINR value, and the variation results from different interference distributions. Based on the observations, we identified several attributes that influence the interference perceived by a pair of transmitting and receiving stations, and developed a

modeling and simulation framework for investigating and emulating the possible types of wireless interference in multi-hop wireless ad-hoc networks. In the proposed framework, there are several control parameters to manipulate the interferences, which will be discussed in Section 4. The simulation results indicated that the proposed framework produces wireless interferences realistic enough to enable examination of the effects on other wireless networking systems. We also found that we should not rely solely on the SINR value to choose the best link among candidates.

The main contributions we made in this paper are as follows. Firstly we presented that the SINR value is not the best criterion to determine the link state, but its distribution during the period of one frame reception actually decides the state. We then devised a modeling and simulation framework for producing realistic wireless interferences to investigate their effects on wireless networks and systems. This is because, even though the SINR distribution determines the link state, the distribution is difficult to be discovered and also is not well fit for any mathematical distribution.

The paper is organized as follows. We briefly explain preliminary knowledge about the IEEE 802.11 physical and MAC layer, together with fundamental relationships between FDR and SINR in Section 2. In Section 3, we present the specific scheme for quantizing interference to discover the relationships between FDR and SINR in detail. Then we propose a simulation framework with control parameters, and also present various results of the proposed framework in Section 4. Finally, we conclude this paper with Section 5.

2. Preliminary

In this section, we briefly summarize IEEE 802.11, which consists of the MAC and physical protocol, in order to give the background knowledge needed for this paper. In the case of the MAC protocol, we do not include any extensions, such as QoS provisioning, power reports, or mesh functions, and in the case of the physical layer, we only explain IEEE 802.11a among several candidates, such as IEEE 802.11 legacy, 802.11b, 802.11g, and 802.11a, due to the space limit.

2.1 IEEE 802.11 MAC and Physical Layer

IEEE 802.11 [12] provides two access methods: (*i*) the Distributed Coordination Function (DCF), also known as the basic access method, is a carrier sense multiple access with collision avoidance (CSMA/CA) protocol; and (*ii*) the Point Coordination Function (PCF) is an access method similar to a polling system that uses a point coordinator to arbitrate the access rights among nodes. In addition, the standard includes a floor acquisition mechanism, consisting of request to send/clear to send (RTS/CTS), to solve the hidden terminal problem.

Since the MAC layer processes only the successfully-received frames regardless of aforementioned access modes, total number of successful transmission in a given interval determines the protocol capacity of the MAC layer. In addition, the successful transmission depends on the SINR value of the received frame. Therefore, SINR values perceived at the physical layer consequently determines the MAC layer capacity.

As mentioned, we focus on IEEE 802.11a physical layer [13] in this paper, but there are similar trends in other types of physical layers. IEEE 802.11a uses four modulation schemes; BPSK, QPSK, 16QAM and 64QAM. As shown in **Fig. 1**, any PHY layer-frame starts with PLCP a preamble to inform a receiver of its arrival. If the PLCP preamble is not recognized or the PLCP header is not correctly recognized by the receiver, the receiver simply ignores the

frame. Otherwise, the receiver continuously reads the PLCP header and then determines the transmission rate (at which the remaining frame is transmitted) and payload size (which determines the end of the received frame). Then, the receiver continues receiving the remaining PLCP frame, by using both the size and rate specified in the PLCP header, even if some interference occurs during reception, and delivers the frame to its MAC layer.

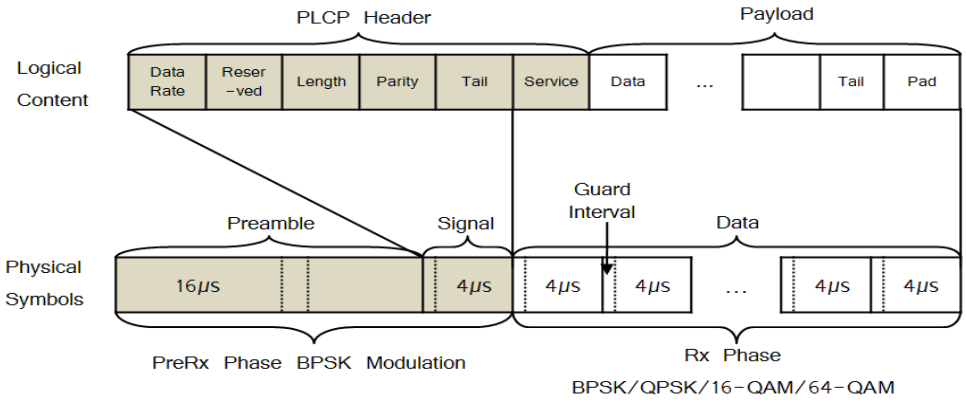

Fig. 1. IEEE 802.11a frame format.

The PLCP preamble and header are supposed to be modulated using BPSK at 6Mb/s, which is the most robust modulation scheme, but the PLCP payload can be modulated with any modulation scheme at any data rate [13]. The modulated PLCP payload is then concurrently transmitted over 48 sub-carriers according to the OFDM design specification.

2.2 BER-SINR relationship in BPSK

Assuming an AWGN (Additive White Gaussian Noise) channel, the bit error rate (BER in the case of BPSK) is given by:

$$BER = 0.5 \times erfc\left(\sqrt{\frac{P_r \times W}{N \times f}}\right) \tag{1}$$

where P_r is the received power, W the channel bandwidth, N the noise power, f the transmission bit rate, and erfc the complementary error function [14]. Based on (1), we know that BER is a function of SINR (P_r /N).

Based on (1), we can also determine the frame error rate (FER) with the given frame length assuming i.i.d.:

$$FER = 1 - (1 - BER)^L \tag{2}$$

where L is the frame length.

According to (1) and (2), we can only determine FER by using SINR and the frame length. Fig. 2 presents the FDR-SINR relationship based on (2) when the frame size is 548 bytes. We observe that there is a sharp separation between the link state of unsuccessful delivery (when FDR is about 0.0) and the other state of successful delivery (when FDR is about 1.0).

3. Interference Estimation

In this section, we explain the method of accurately calculating the interference for each received frame at the physical layer, which uses the physical layer model proposed by Q. Chen et al. [15]. Then we perform a simulation study to verify if our simulation results are similar to the analytical results in **Fig. 2**.

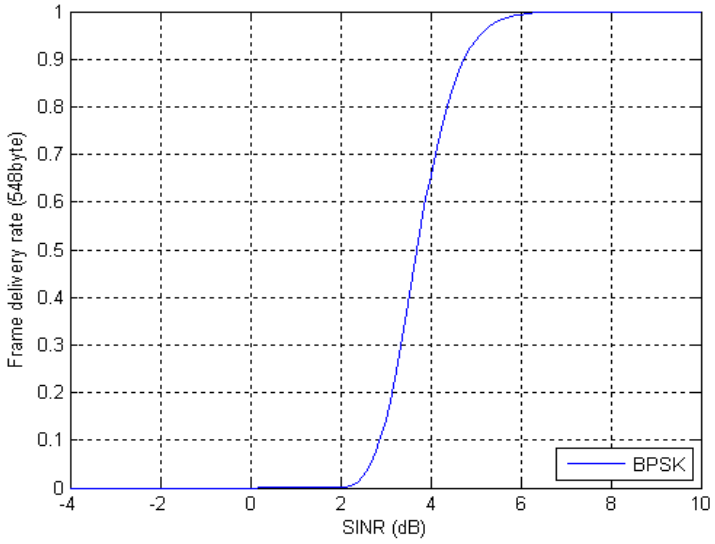

Fig. 2. Theoretical relationship of FDR and SINR

3.1 Calculating the Frame Delivery Rate

When frames arrive at wireless stations, they are detected, recognized, and monitored for their accumulated power level. When a frame arrives at a station in idle mode, the station decides whether or not it can continuously receive the frame by examining the PLCP header, as explained in the previous section. During the frame reception, the station continues monitoring the power level of the frame, in order to determine its received signal strength (RSS), such that the total accumulated power for the whole frame is divided by the frame length. Note that there may be some interference at any time during the frame reception, and the physical layer cannot recognize such interference, and even if it perceives the interference, it cannot determine how many interfering stations contribute to the interference.

In multi-hop wireless ad-hoc networks, we cannot expect all the stations to be synchronized, since there is no centralized infrastructure. So, two or more transmissions may interfere with each other within the period of one frame transmission. Therefore interference is not identical in terms of the strength and duration during this period, which means that each interfered section within one frame may have a different FDR. **Fig. 3** shows one example of such a case. In the figure, there are four different intervals of interference for the received frame, each of which has a different error rate.

Therefore, we need to separately compute Frame-Error-Rate (FER), where FER=1-FDR, for each section, in order to correctly determine the total FER for the whole frame. The specific procedure for determining the FER is as follows: (*i*) We compute BER with SINR for each section using (1); then (*ii*) We calculate FER for the section with the frame length using (2); (*iii*) We finally determine the FER for the whole frame with different FERs for different sections. The example in **Fig. 3** can be expressed by:

$$FER = 1-(1-ER_a)\times(1-ER_b)\times(1-ER_c)\times(1-ER_d) \quad (3)$$

where L is the frame length, ER_a is the FER for section a, ER_b is the FER for section b, ER_c is the FER for section c and ER_d is the FER for section d. The total FER, as in (3), is used to determine whether the received frame is corrupted, once it has been completely received at the receiver.

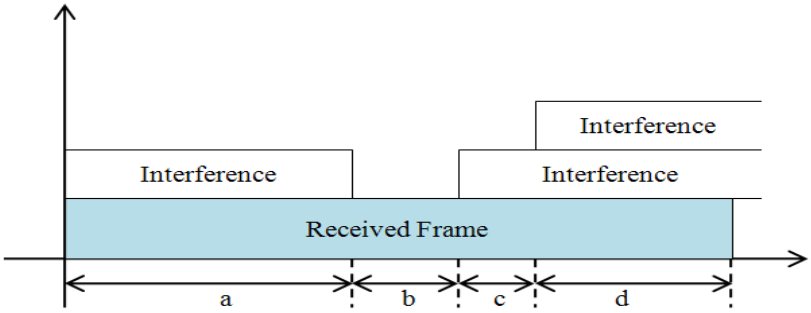

Fig. 3. An example of intra-frame interference for FER calculation

3.2 Extending the Simulation Tool

We enhanced *ns*-2 *rev* 2.33, to accommodate the previous scheme of interference calculation for correctly emulating frame receptions at the physical layer. Based on this extension to the physical layer, we performed a simulation study using the simple topology in **Fig. 4** to measure the real-world characteristics of interference. This consisted of 16 stationary stations where each station has three to five neighboring stations (which may cause interference). In order to conveniently compute the relationships between FDR and SINR, we introduced a *measurement interval,* which is set to one second in this paper. In every measurement interval, we measured the average power of interference at each link, and also determined that of the received frame, using only the path loss and propagation model (since stations are stationary). Thus, we can calculate SINR for every measurement interval, using the noise floor (assumed to be constant), received signal power, and average interference power. Consequently we can compute FDR.

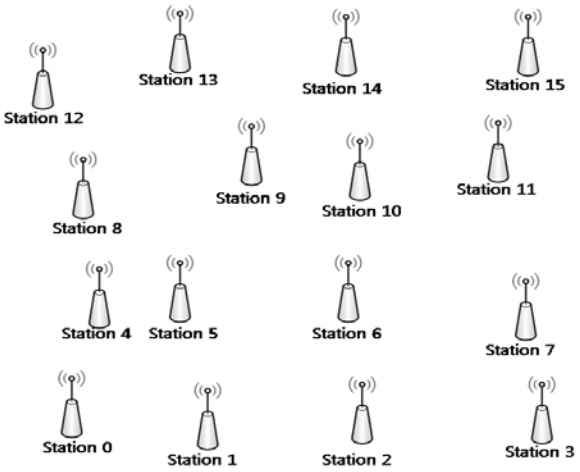

Fig. 4. A network topology for simulation

Fig. 5 presents the FDR-SINR relationships obtained from the aforementioned simulation study. In the figure, each color and mark represents the results obtained at each link (which is determined by the pair of transmitting and receiving stations). As indicated in the figure, the relationships do not have the same sharp distinction where there is narrow range of SINR values between successful and unsuccessful delivery, as shown in **Fig. 2**.

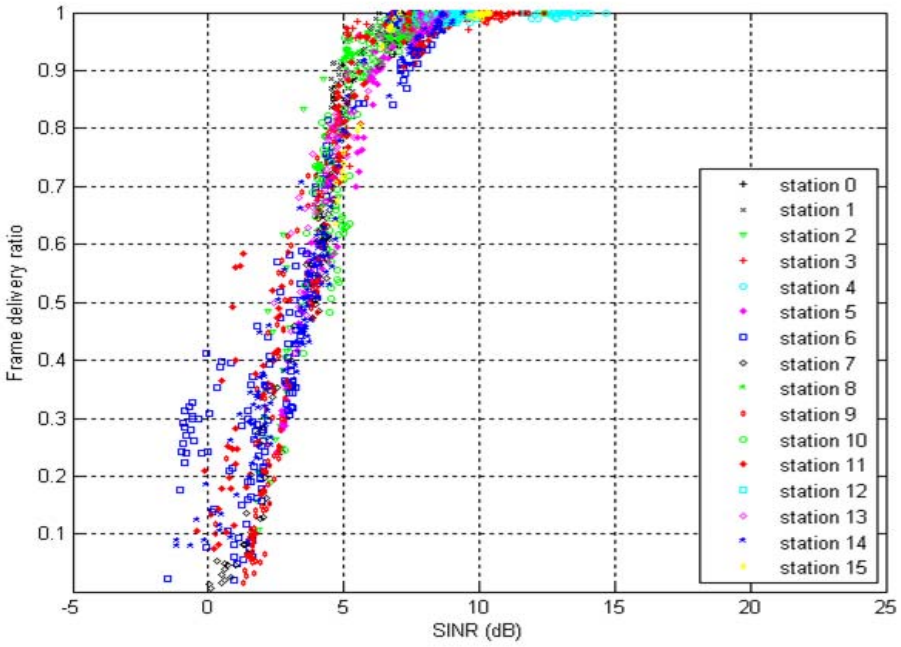

Fig. 5. Relationships between FDR and SINR measured from the topology presented in **Fig. 4**

It is interesting to note that the figure shows that even one station has several different relationships between FDR and SINR. Especially, we observe that two links with the same SINR value can have different FDR values. For example, the link from station 11 (transmitter) to station 10 (receiver), which is denoted by α, and the link form station 6 (transmitter) to station 10 (receiver), which is denoted by β, in the network of **Fig. 4**, have different FDR values, even though they have almost the same SINR values. We investigated this case further. **Fig. 6** presents two distributions of interference and their corresponding SINR values that we observed from the simulation for all the frames observed at the two links. We determined that since the two links have different interference distributions, even though they have similar SINR values (5.03dB and 5.04dB respectively), they have different FDR values. In detail, the interference values observed at link α (**Fig. 6** (a)) are more concentrated at the average value, while the values measured at link β (**Fig. 6** (b)) are widely distributed across high and low interference values. Additionally, most of the SINR values presented in **Fig. 6** (a) are high enough to be correctly decoded at the receiving station, but the values shown in **Fig. 6** (b) are distributed over a wide range of SINR values, including SINR values too low to be decoded at the station. We conclude that links with the same SINR value can have different FDR values, due to different distributions of interference.

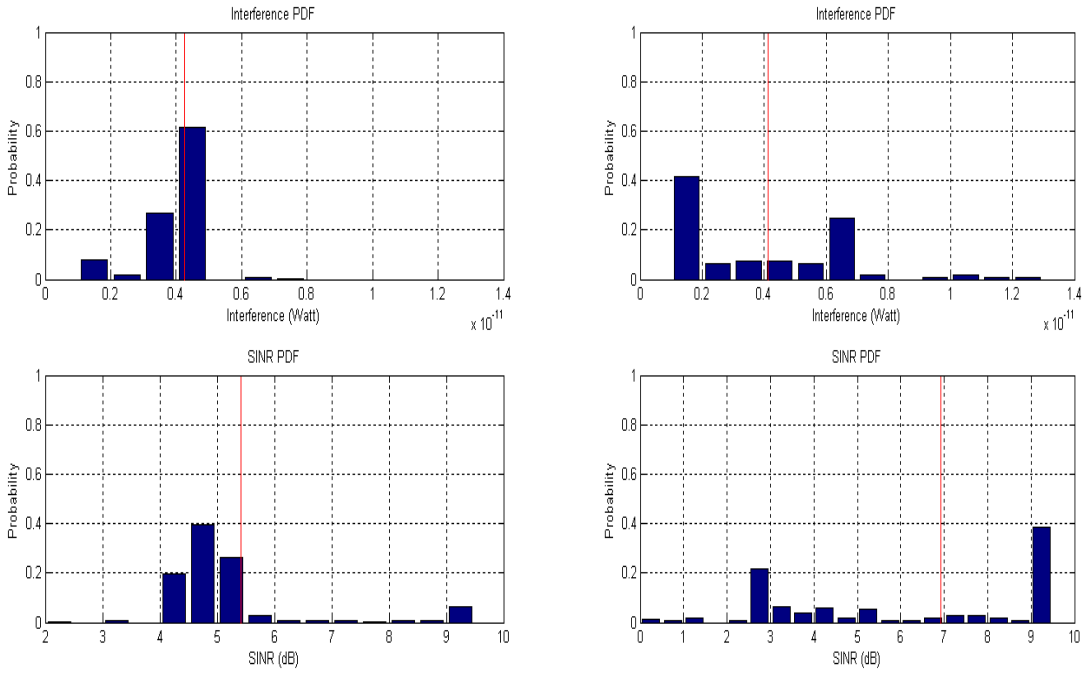

(a) link α (b) link β

Fig. 6. Distributions for interference and its corresponding SINR for two links α and β, both with the same SINR but different FDR

4. Interference Modeling and Simulation

In this section, we present an interference model that determines the possible range of SINR values, which are restricted by both an upper and lower bound according to the number of interfering stations. Based on the model, we implemented a simulation framework and performed enough simulations to inspect various effects of wireless interference and determine whether or not the framework accurately emulates the results presented in **Fig. 5**.

4.1 Identifying Interference Distance

In order to produce interference for on-going transmission, we needed to ensure that the transmitting and interfering stations can simultaneously transmit their frames, by locating each beyond the carrier sense range of the other. The reason is that if one is within the other's carrier sense range, it simply defers its transmission, thus, it does not produce any interference. For the maximum interference, we used the following procedure to determine the location for each interfering station, for a given number of interfering stations. Since the *carrier sense threshold* value is assumed to be constant, the number of interfering stations is regarded as the main parameter determining the carrier sense range. We first calculated the carrier sense range for each given number of interfering stations. We know that the maximum number of interfering stations is six[1], according to [16] and [17], and the RSS of the received frame can be

[1] This number of interfereing stations dominate to interfere with on-going transmission of a pair of transmitting and receiving stations (see [16] and [17]).

determined by the transmission power P_t , communication distance d, and a chanel gain κ:

$$P_r = \frac{P_t \times \kappa}{d^2} \tag{4}$$

Interference recognized by a transmitting station is thus determined as:

$$CSThreshol\ d = \frac{P_t \times \kappa}{d_1^{\ 2}} = 2 \times \frac{P_t \times \kappa}{d_2^{\ 2}} = 3 \times \frac{P_t \times \kappa}{d_3^{\ 2}} = 4 \times \frac{P_t \times \kappa}{d_4^{\ 2}} = 5 \times \frac{P_t \times \kappa}{d_5^{\ 2}} = 6 \times \frac{P_t \times \kappa}{d_6^{\ 2}}, \tag{5}$$

where d_1, d_2, d_3, d_4, d_5, and d_6 denotes the distance between the transmitting station and interfering stations when the number of the stations is 1, 2, 3, 4, 5, and 6, respectively.

Based on (5) we can determine the relationship among carrier sense ranges as:

$$d_1 = \frac{d_2}{\sqrt{2}} = \frac{d_3}{\sqrt{3}} = \frac{d_4}{\sqrt{4}} = \frac{d_5}{\sqrt{5}} = \frac{d_6}{\sqrt{6}}. \tag{6}$$

Since we needed to place interfering stations at the boundary of the carrier sensing range, in order for a receiving station to receive the maximum interference, we used the above carrier sense range to locate interfering stations.

Fig. 7 presents six types of wireless network topologies, each of which has between one and six interfering stations. Based on these topologies, we first computed the relationship between the SINR and distance (between a pair of transmitting and receiving stations) for the given number of interfering stations. **Fig. 8** presents these results. Then, we determined the range of SINR values, which are restricted by both the maximum and minimum values of SINR. The maximum SINR can easily be determined when there is no interfering station, and the minimum SINR can be determined using the results in **Fig. 8**. Note that based on **Fig. 8**, the lower bound of SINR increases as the number of interfering stations increases.

4.2 Interference Factors

As is well-known, it is hard to accurately emulate interference characteristics, since we cannot enumerate all the factors resident in extremely dynamic and unpredictable radio environments: for example, interfering stations may be located at any position relative to the transmitting or receiving station and their aggregate transmission rate varies from time to time. Therefore, we first identify the important factors based on simulations, and then devise an interference framework with the relationships between SINR and distance in **Fig. 8**. Within this framework, we manipulate the control parameters to produce realistic wireless interference:

1) *Number of interfering stations*: Since we need a communication configuration where interference disturbs the receiver to receive a frame, we should locate interfering stations away from the transmitter, to avoid the deferrence of its transmissions. In order to control the number of interfering stations in the framework, we choose one of the six possible configurations presented in **Fig. 7**, and then we locate them in the network, to generate the maximum interference with on-going transmissions;
2) *Active interfering station*: Even though we choose one of six possible scenarios in terms of the number of interfering stations, it seems to be unrealistic to enable all chosen stations to be active. The reason is that if we enabled all selected interfering stations to simultaneously transmit their frame, the receiving station would only have the minimum SINR, as indicated in **Fig. 8**. Therefore, we turn on/off the selected interfering stations

with different probabilities in the framework, which actually produces an intermediate level of interference, as mentioned in Section 2;

3) *Angle between a pair of transmitting and receiving stations*: The locations of the receiving stations presented in **Fig. 7** are chosen such that the maximum interference occurs. Since this does not seem realistic, we randomly determine the angle between the pair of transmitting and sending stations with $1/2\pi$ probability in the framework.

4.3 Simulation Study

Based on the observations in Section 3 and the subsequent interference model, we realized an interference framework in the MATLAB, in order to examine interference and its effects on wireless neworks. Then, we conducted a set of simulations that generates dynamic wireless interferences, and we observed various occurrences and effects of the interference.

For each simulation scenario, we measured SINR and FDR in each measurement interval (one second). We changed the distance between the transmitting and receiving stations from 100m to 240m, in increments of 20m. We set the number of frame transmissions (whose length is 548 bytes where 48 bytes are used for IP and MAC header) to 500 for each measurement interval (about 2Mb/s). Note that the reason that we set the minimum distance to 100m is that the minimum SINR is high enough to successfully decode the received frame within a distance less than 100m.

Performance evaluation in the presence of th maximum interference: For the first simulation study, we fixed the angle between a pair of transmitting and receiving stations to have a configuration where the maximum interference occurs. But, we changed the other two control parameters: (*i*) We changed the number of interfering stations every second, which means there was no change in the number of interfering stations for one measurement interval, or that number was changed every frame transmission, resulting in 500 changes every second; (*ii*) We changed the number of active interfering stations.

Fig. 9 shows the results when we fixed the number of interfering stations for one second. Recall that in this configuration, the number of interfering stations remains constant, while 500 frames are transmitted. **Fig. 9** (a) shows the simulation results when the interfering stations are set to be turned on/off with 0.5 probability, and **Fig. 9** (b) presents the results when we turn on all interfering stations. In both figures, we observe that the relationships in **Fig. 9** are closer to the theoretical curve of the SINR-FDR relationships in **Fig. 2**.

Fig. 10 presents the simulation results when we changed the number of interfering stations in every frame transmission. **Fig. 10** (a) presents the SINR-FDR relationships when we turned on/off each interfering station with 0.5 probability. **Fig. 10** (b) shows the results when all interfering stations are turned on. As observed in **Fig. 9** (b), the results in **Fig. 10** (b) are very close to the theoretical results of the SINR-FDR relationship. Thus, we conclude that the receiving station receives the maximum interference from interfering stations only when all interfereing stations are turned on, since the theoretical values are generated in those cases.

Performance evaluation in the cases when we change relative positions between a pair of trnasmitting and receiving stations: For the second simulation study, we relaxed the constraint that the angle between a pair of transmitting and receiving stations is fixed, and thus we changed the angle in each frame transmission. Note that even though we changed the angle, this can be considered as changing the positions of interfering stations, and thus we expected to obtain a wider range of interference values (as perceived by the receiver). For this simulation study, we employed the configurations used in **Fig. 9** (a) and **Fig. 10** (a) after we changed the angle parameter, but we did not use the configurations in **Fig. 9** (b) and **Fig. 10** (b),

since they produced results that are far from desirable.

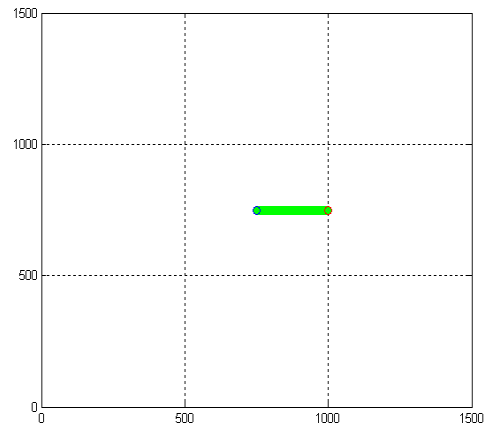

(a) # of interferers =1

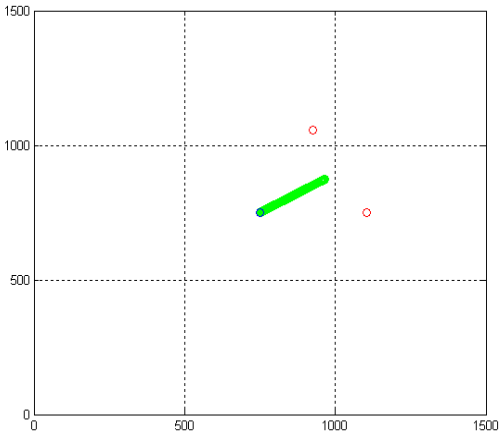

(b) # of interferers =2

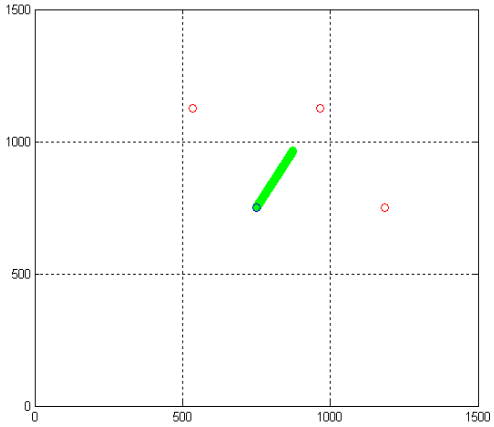

(c) # of interferers =3

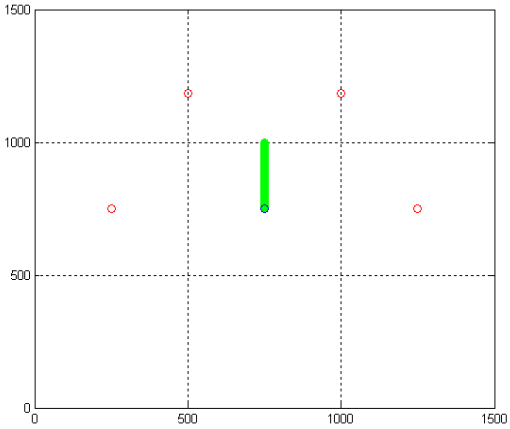

(d) # of interferers =4

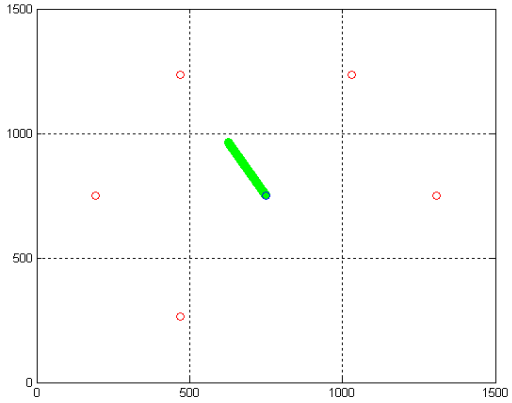

(e) # of interferers =5

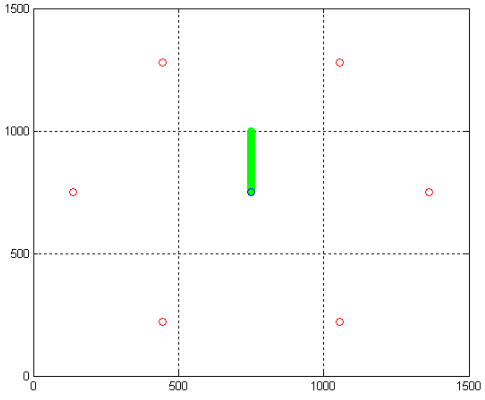

(f) # of interferers =6

Fig. 7. Six topologies with various numbers of interfering stations

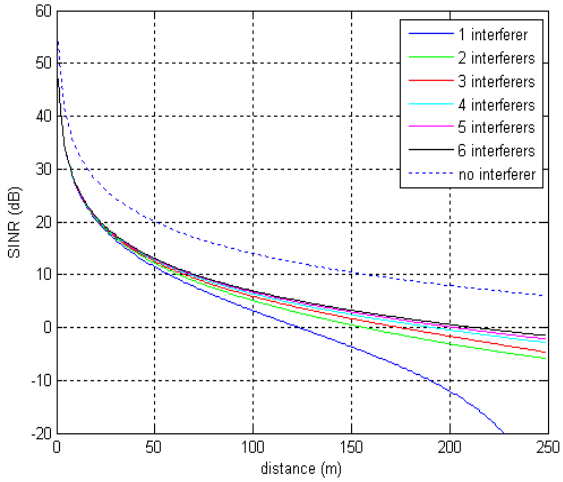

Fig. 8. Relationship between SINR and distance

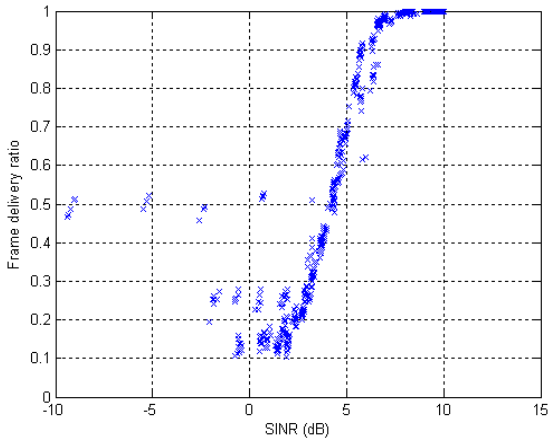

(a) Interfering stations are randomly enabled with 0.5 probability

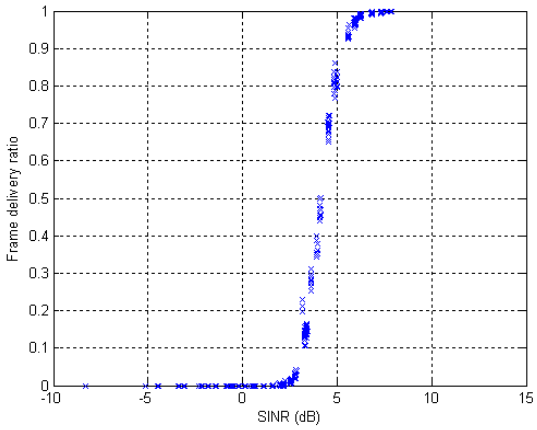

(b) All the interfereing stations are always on

Fig. 9. Relationships between FDR and SINR when the number of interfering stations is fixed for one second

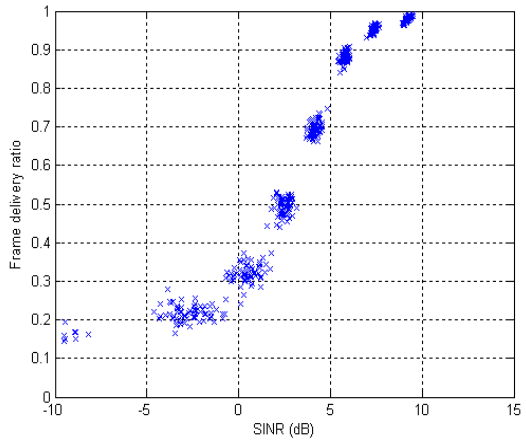

(a) Chosen interfering stations are randomlyy enabled with 0.5 probability

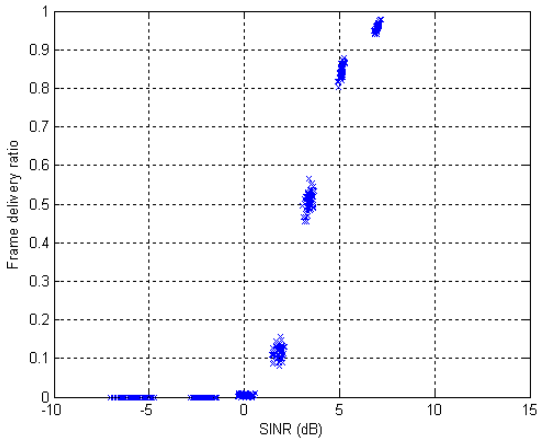

(b) All interfering stations are always on

Fig. 10. Relationships between FDR and SINR when the number of interfering stations is varied for each transmitted frame

Fig. 11(a) presents the results of the FDR-SINR relationship obtained from the same configuration as in **Fig. 9** (a), except that we changed the angle parameter, and **Fig. 11** (b) shows the results when we changed the angle values in the configuration in **Fig. 10** (a). The simulation results in both figures show a wider range of relationships between FDR and SINR, as we expected.

Even though the simulation results in **Fig. 11** shows a much wider range of interferences, there are some atypical cases where the FDR values are very high and the SINR values are less than zero. This is why we do not consider the cases where strong interference arrives at the receiving station before it receives the intended frame, and thus the station cannot hear the preamble of the frame [18]. **Fig. 12** gives an example of the sequence of frame reception that comprise the atypical cases: if interferences *A* and *B* are strong enough to corrupt the received frame, interference *A* prevents the receiving station from detecting the frame, while interference *B* corrupts the payload section of the frame. Therefore, if we excluded such a sequence of frame receptions from the SINR calculation, we would exclude the atypical cases.

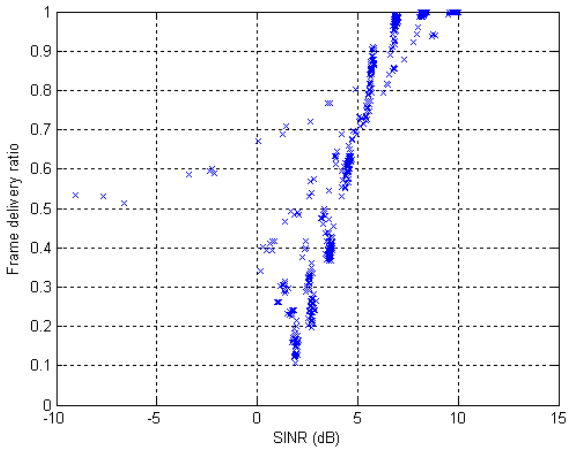

(a) The number of interfering stations is fixed during one second and the interfering stations are randomly enabled with 0.5 probability

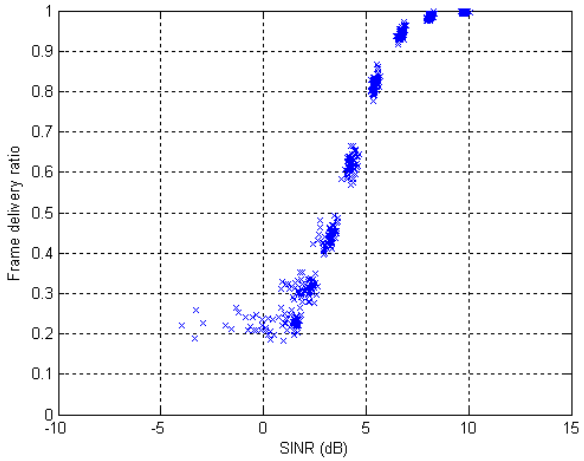

(b) The number of interfering stations is changed during one second and the chosen interfering stations are randomly enabled with 0.5 probability

Fig. 11. Relationships between FDR and SINR measured when we change the angle between a sender and receiver

Fig. 13 (a) and (b) presents the relationship between FDR and SINR values for the same network configuration as in **Fig. 11** (a) and (b), except where we have excluded the atypical cases in **Fig. 12**. It is clear from the figures that the atypical cases are no longer present, and that the SINR-FDR relationships are more realistic.

Performance evaluation in the cases when interfering stations are randomly activated and placed: For the third simulation study, we changed the locations of interfering stations, but we fixed the angle between a pair of transmitting and receiving stations. When we placed the interfering stations, we set the distance between the sender and interfering station such that each was beyond the other's carrier sense range, in order to enable simultaneous communications (or generate interferences), and also ensured that the distance between any pair of interfering stations was such that each was beyond the other's carrier sense range. Additionally, for various simulations, we varied the number of interfering stations from one to

six, and also changed the distance between a pair of sending and receiving stations from 100m to 240m, in increments of 20m. Moreover, we set the transmission rate of a transmitting station to 500 frames per second (about 2Mb/s).

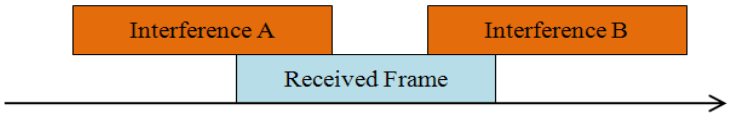

Fig. 12. A timing sequence that produces a high FDR when the SINR is less than zero

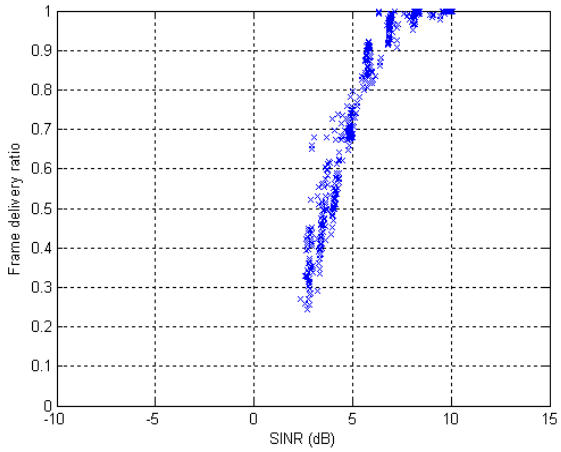

(a) The number of interfering stations is fixed for one second and the interfering stations are randomly enabled with 0.5 probability

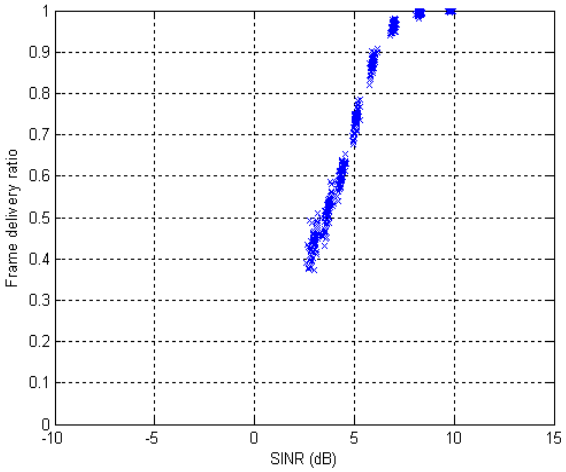

(b) The number of interfering stations is changed for one second and the chosen interfering stations are randomly enabled with 0.5 probability

Fig. 13. Relationships between FDR and SINR measured when we exclude the cases where the receiving station cannot successfully receive the preamble of the received frames

Fig. 14 and **Fig. 15** show the simulation results of the FDR-SINR relationships when we used different probabilities to turn on/off each interfering station. **Fig. 14** shows the results when we turned on/off each interfering station with a randomly chosen probability within the

range of [0.0, 1.0]. **Fig. 15** presents the results when we enabled each interfering station with a randomly chosen probability within the range of [0.3, 1.0] instead of [0.0, 1.0]. From both figures, we observe that a wider range of intermediate FDR values is produced when we control the locations of the interfering stations.

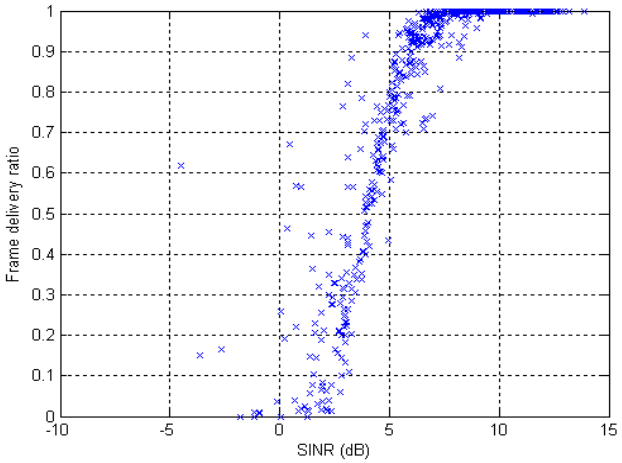

Fig. 14. Relationships between FDR and SINR measured when we change the number of interfering stations and turn on each interfering station randomly with a probability range of [0.0, 1.0]

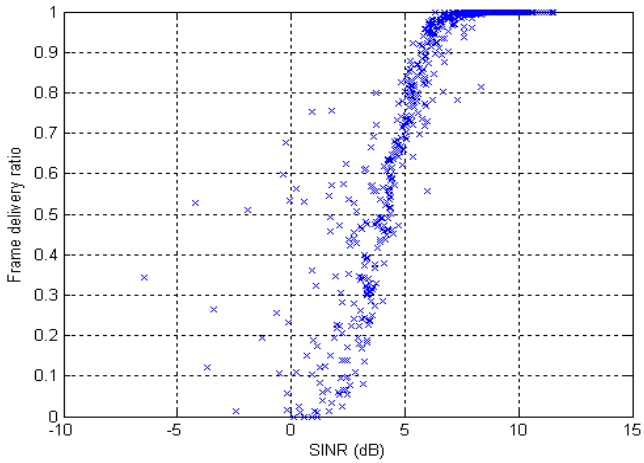

Fig. 15. Relationships between FDR and SINR measured when we change the number of interfering stations and turn on each interfering station randomly with a probability range of [0.3, 1.0]

Performance Evaluation in the cases with different frame sizes: For the forth simulation study, we verified if the proposed framework still works with different frame sizes. We use the same simulation configuration as used for **Fig. 15** (the third simulation). **Fig. 16** presents the relationships between FDR and SINR when we use the different frame size, which is 148 bytes (where 48 bytes are used for IP and MAC header). **Fig. 17** presents the relationships between FDR and SINR when we use the different frame size, which is 1348 bytes. We observed that the frame size does not affect on the results as much as we expect since the frame error rate does not increase as fast as the bit error rate as SINR decreases. Note that the relationships between SINR and FDR shifts right as the frame size increases.

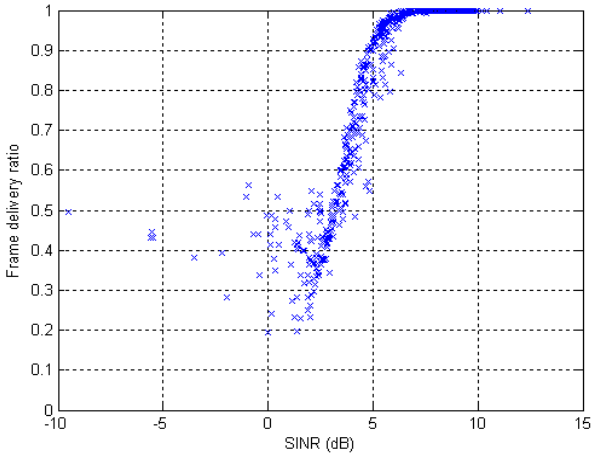

Fig. 16. Relationships between FDR and SINR when we employ the same configuration as used for the results in **Fig. 15** except that the frame size is set to 148 bytes

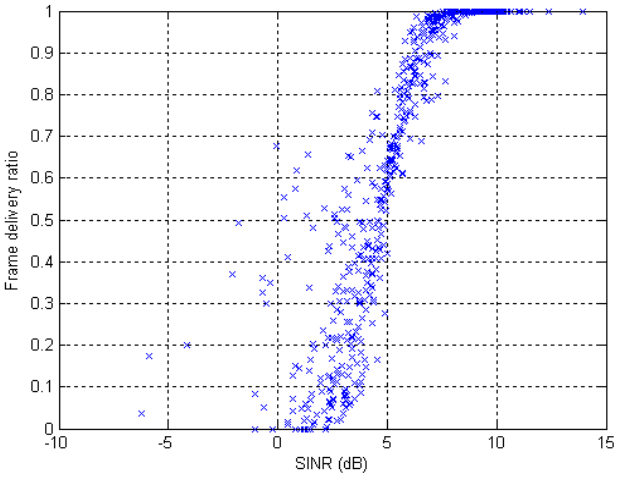

Fig. 17. Relationships between FDR and SINR when we employ the same configuration as used for the results in **Fig. 15** except that the frame size is set to 1348 bytes

Performance evaluation in the cases with different channel rate: For the fifth simulation study, we employed two different channel rates, 12 Mb/s and 24 Mb/s, instead of 6 Mb/s. Since modulation schemes at 12Mb/s and 24Mb/s are QPSK and 16-QAM, respectively, in IEEE 802.11a, we need to use other BER equations than (2). In QPSK modulation, BPSK is used in modulating both the in-phase and the quadrature-phase component of the carrier, and so, BER for QPSK is the same as that for BPSK. In 16-QAM modulation, BER is given by:

$$\text{BER} = \frac{2}{4} \times \left(1 - \frac{1}{\sqrt{16}}\right) \times Q\left(\sqrt{\frac{3k}{16-1} \times \frac{P_r \times W}{N \times f}}\right) \tag{7}$$

Fig. 18 presents the FDR-SINR relationships when the frame size is 548 bytes, and **Fig. 19** shows the simulation results when the channel rate is 12 Mb/s, the frame size is 548 bytes, and the same configuration as used for **Fig. 15** is used. **Fig. 20** presents the FDR-SINR relationships based on (7) when the frame size is 548 bytes, and **Fig. 21** shows the simulation results when the channel rate is 24 Mb/s, the frame size is 548 bytes, and the same

configuration is used.

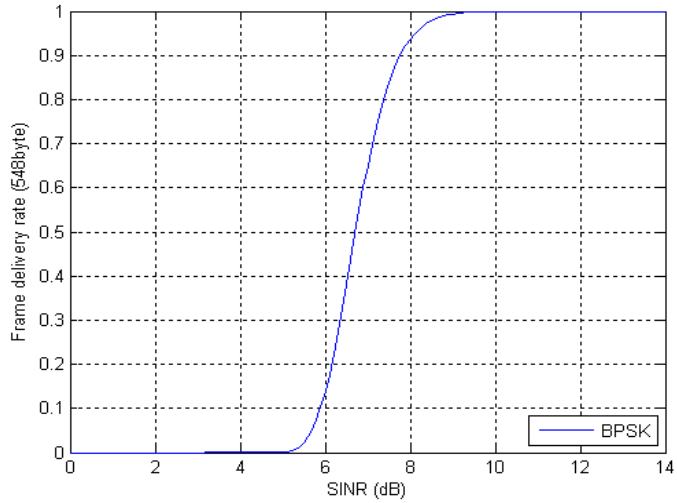

Fig. 18. Theoretical relationship between FDR and SINR when we use 12 Mb/s as the channel rate and 548 bytes as the frame size

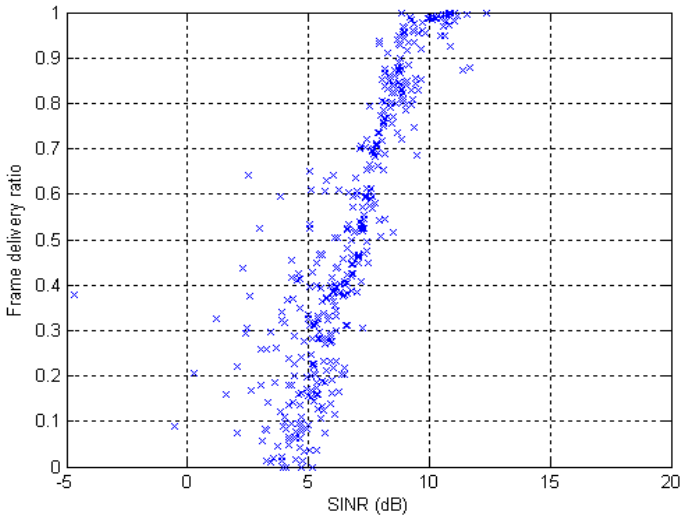

Fig. 19. Relationships between FDR and SINR when we set the channel rate to 12 Mb/s, the frame size to 548 bytes, and we employ the same configuration as used for the results in **Fig. 15**

Performance evaluation in the case when transmission rates of interfering stations follows a Poisson distribution: As the sixth simulation, we set the transmission rate of each interfering station to be distributed over a Poisson distribution after it is activated. We basically use the same simulation configuration as used for the results in **Fig. 15.** We have two scenarios for this study. In the first scenario, all interfering stations are assumed to use the same transmission rate when they are enabled. **Fig. 22** presents the FDR-SINR relationships for this scenario. In the other scenario, all interfering stations are set to have different transmission rates in the range from 0 to 1000 frames per second according to the Poisson distribution. **Fig. 23** shows the results in this case.

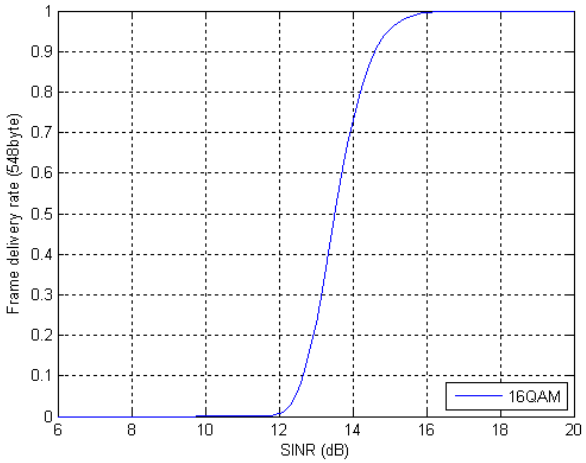

Fig. 20. Theoretical relationship between FDR and SINR when we use 24 Mb/s as the channel rate and 548 bytes as the frame size

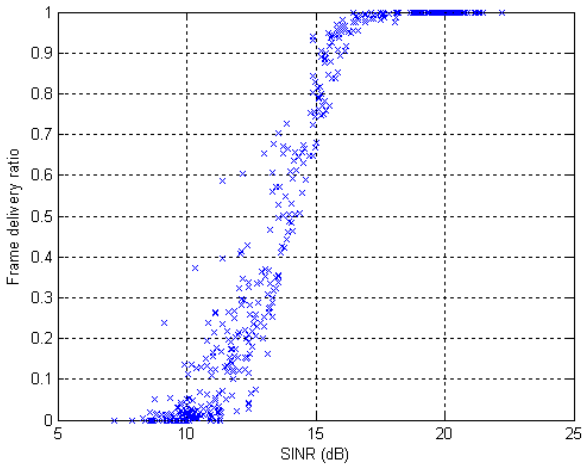

Fig. 21. Relationships between FDR and SINR when we set the channel rate to 24 Mb/s, the frame size to 548 bytes, and we employ the same configuration as used for the results in **Fig. 15**

Performance evaluation in the presence of mobility: As the last simulation, we analyzed the effect of mobile station on the relationships between FDR and SINR. We established a mobile scenario for one receiving station, such that the receiving station simply takes a random step from its last position from one period to the next and uses a different pair of speed and direction for each period. This is the so-called "random walk" model.

The moving scenario of the receiving station is presented in **Fig. 24**, where the pink solid line denotes the transmission range of the transmitting station and the blue solid line is the trajectory of the mobile station. **Fig. 25** presents the results when we used the same simulation configuration as used for the results in **Fig. 15**. We observe that the mobile pattern of the receiving station merely changes the number of interfering stations in the proximity of the receiving station.

Insights on the simulation results: Based on the simulation results, we define the following evaluation metrics to analyze characteristics of wireless interferences:

- Factor A = mean $\left((\text{avg}(sir)-\text{std}(sir))^2\right)$, for $\forall sir \in S_{SINR}$,
- Factor B = mean $\left(\text{val}(sir)\right)$, for $\forall sir \in S_{SINR}$,
- Factor C = mean $\left((\text{std}(dst))\right)$, for $\forall dst \in S_{DIST}$,

where

- avg(*sir*): the average of FDR value at around the *sir*,
- std(*sir*): the standard deviation of FDR value at around the *sir*,
- val(*sir*): the theoretical value of FDR at the *sir*,
- std(*dst*): the standard deviation of SINR value obtained at *dst*, which denotes the distance between the transmitting and receiving stations,
- S_{SINR}: the set of measured *sir* values from the minimum to maximum value in increments of 0.2dB interval,
- S_{DIST}: the set of distances (*dst*) between the transmitting and receiving stations.

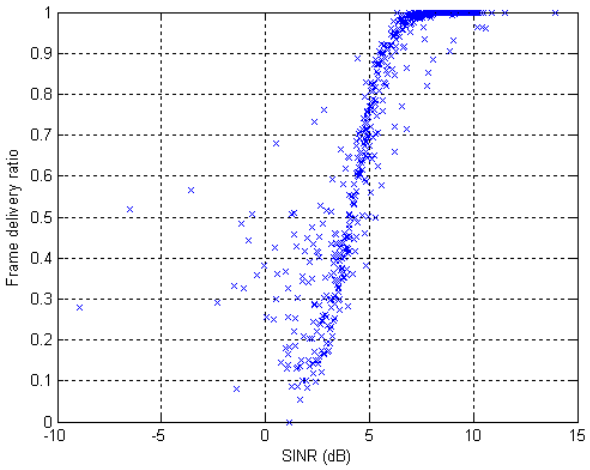

Fig. 22. Relationships between FDR and SINR when we enabled each interfering station with the same transmission rate according to a Poisson distribution

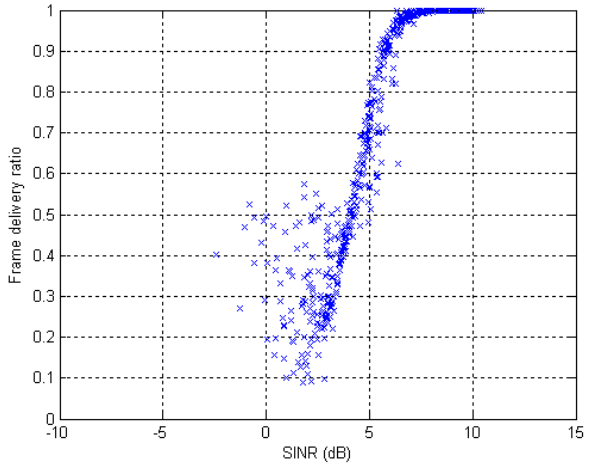

Fig. 23. Relationships between FDR and SINR when we enabled each interfering station according to a Poisson distribution

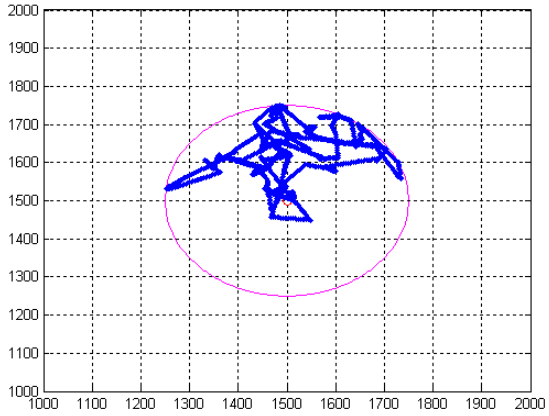

Fig. 24. The mobile trajectory of the receiving station

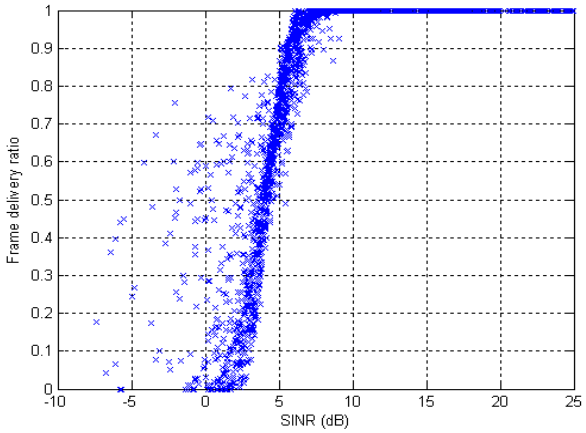

Fig. 25. Relationships between FDR and SINR measured when the receiving station is mobile, and the simulation configuration as used in **Fig. 15**

Factor A denotes to what extent measured FDR is close to its corresponding theoretical value. The smaller Factor A means that there is smaller discrepancy between measured and theoretical values. Factor B represents how wide a range of SINR values can be obtained in a simulation. The higher Factor B means the wider range. High Factor B values were obtained from the simulation that we activated interfering stations randomly. Factor C represents the degree of variances in wireless interference perceived by the receiving station. The specific analysis on the simulation results is presented in **Table 1**. We do not include all the analysis due to the space limit.

Table 1. Analysis on simulation results.

Simulation results	Performance metrics		
	Factor A	Factor B	Factor C
The results at **Fig. 9** (a)	0.0600	0.0189	2.3358
The results at **Fig. 10** (a)	0.0572	0.0113	1.9659
The results at **Fig. 11** (b)	0.0400	0.0151	2.0262
The results at **Fig. 13** (b)	0.0282	0.0133	1.9268
The results at **Fig. 14**	0.0196	0.0440	4.2857
The results at **Fig. 15**	0.0406	0.0600	2.7923

The results at **Fig. 22**	0.0439	0.0472	2.3895
The results at **Fig. 23**	0.0374	0.0519	2.3541

4.4 Application

Based on all the simulation results in the previous section, we observe that a wireless link with a higher SINR value does not always guarantee a higher FDR: it has been shown that even if a wireless link has a higher average interference value than other links, the link may have a higher FDR depending on interference distributions. In this section, we briefly introduce a means to use this property (or the proposed framework) with a simulation.

We used the network topology in **Fig. 26** for this simulation. In the figure, there are two APs connected to the Internet and six stations, from which we choose one station (denoted station) to investigate the FDR-SINR relationships. The other five stations are assumed to interfere with station's transmissions, and are beyond each other's carrier sense range and that of the station's. The two APs are equally distant from the station, so that they observe the same RSS for frames transmitted by the station. The station transmits 500 frames for one second during the whole simulation time of 64 seconds. Additionally, we used the probability range [0.0, 1.0] to selectively turn on each interfering station. We measured the SINR, FDR, and the average and standard deviation of the interference at the link connected to AP 1 (denoted by *link 1*) and the link connected to AP 2 (denoted by *link 2*).

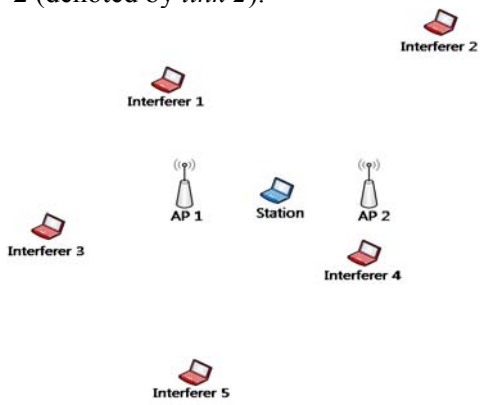

Fig. 26. An example topology for an application of the proposed scheme

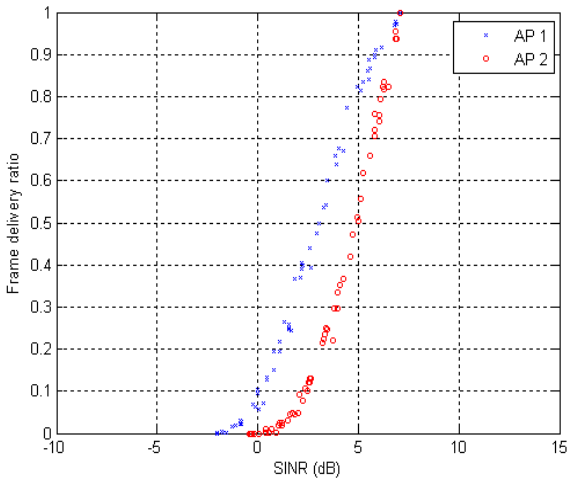

Fig. 27. FDR vs. SINR relationships measured in the topology of **Fig. 26**

Fig. 27 compares the FDR-SINR relationships of *link 1* compared with the values of *link 2*. Based on the figure, *link 2* requires a higher SINR value than *link 1* for a given FDR value.

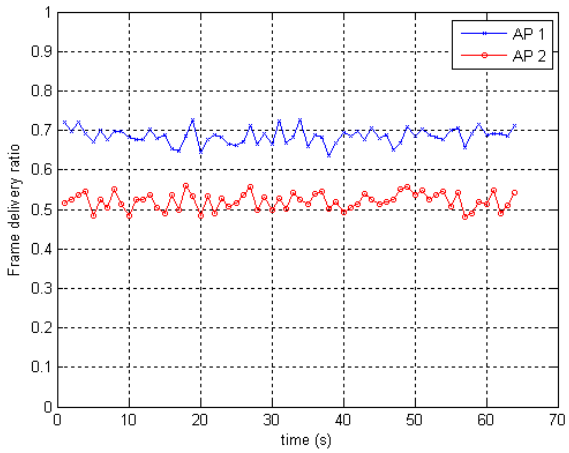

(a) FDR dynamics

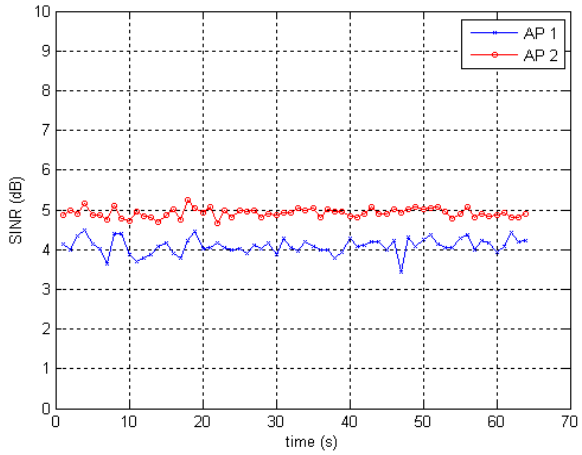

(b) SINR dynamics

Fig. 28. Time-varying fluctuation of FDR and SINR values

In order to investigate the relationship, we measured the time-varying changes of both the FDR and SINR values in the simulation time. **Fig. 28** (a) and (b) present the FDR and SINR changes, respectively. Note that in both figures, *link 2* has higer SINR values than *link 1* throughout the simulation time, but it has lower FDR values than *link 1*. In order to discover the exact reason for this, we measured the average and standard deviation of the interference at the two links, which is presented in **Fig. 29**. Caution is required in interpreting the two figures in **Fig. 29**. Note that *link 1* has higher interference than *link 2* (see **Fig. 29** (a)), and it has a higher standard deviation than *link 2* (see **Fig. 29** (b)). This result does not conflict with the results of **Fig. 28**. This is because *link 2* has steady interference, since it has a steady standard variation, thus, the interference remains around the average interference value, with less fluctuation than *link 1*. On the contrary, *link 1* has some periods of good states (lower interference) and other periods of bad states (higher interference) because of the higher standard deviation presented in **Fig. 29** (b). Thus, a higher FDR in good states compensates for

a lower FDR in bad states, which results in a higher FDR on average, as shown in **Fig. 28** (a).

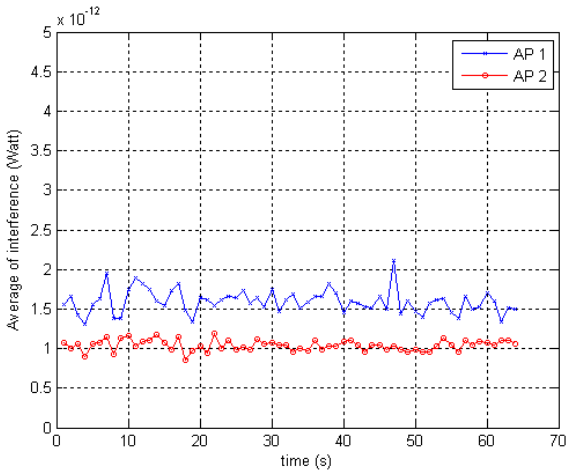

(a) Average interference

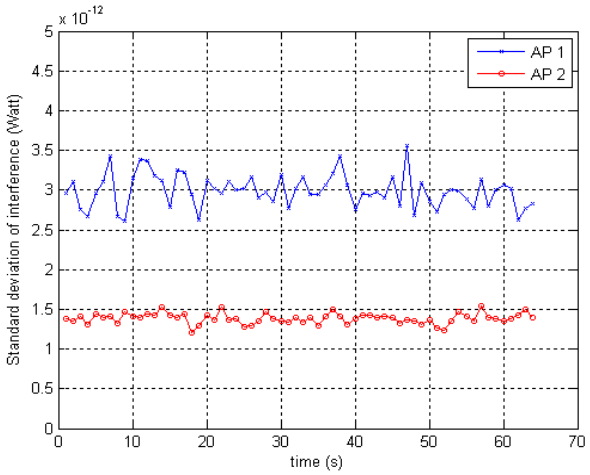

(b) Standard deviation of interference

Fig. 29. Average and standard deviation of interferences

We can state that it is not always a good strategy to choose a "good" link based only on the SINR value, without considering any other parameters. Therefore, we expect that if a wireless station is equipped with the proposed framework, it could choose a better link in terms of FDR rather than SINR, which was proved to be better based on all the simulations introduced in the previous sections. Note that many link-aware protocols, such as the hand-off scheme or routing protocols, use an SINR value or a sequence of SINR values as the most important criterion for selecting the best link among several candidate links connected to neighboring stations (other stations or APs).

5. Conclusion

Many empirical works have presented that there is no sharp distinction of SINR values that can separate the good link state of successful delivery and the bad link state of unsuccessful

delivery. Motivated by such work, we carried out a simulation study to investigate the underlying characteristics of wireless interference, which incur an intermediate range of SINR values. We then devised an interference model to accurately calibrate wireless interferences. We also constructed a simulation framework with several control parameters, which were used for further investigation on wireless interference. Based on the simulation framework, we conducted an extensive simulation study, by changing a wide range of control parameter values. The simulation results indicated that the proposed framework produces more realistic wireless interferences and can be used to analyze the impact of the interferences on other network protocols in multi-hop wireless ad-hoc networks. It also presented that we should not rely only on the SINR value to choose the best link among one or more candidate links.

We identify several works as future work. We plan to enhance the proposed interference model and framework to accommodate a more elaborate set of control parameters, and incorporate them into various simulation tools. We would also like to exploit the proposed framework to improve the service quality of other wireless protocols and systems, by enabling them to choose better wireless links.

References

[1] D. Aguayo, J. Bicket, S. Biswas, G. Judd and R. Morris, "Link-level Measurements from an 802.11b Mesh Networks," in Proc. of *ACM SIGCOMM 2004*, Portland, Oregon, USA, Aug. 2004.

[2] D. S. J. De Couto, D. Aguayo, B. A. Chambers, R. and Morris, "Performance of Multihop Wireless Networks: Shortest Path is Not Enough," in Proc. of *ACM SIGCOMM 2003*, vol. 33, no. 1, pp. 83-88, Jan. 2003.

[3] D. S. J. De Couto, D. Aguayo, J. Bicket and R. Morris, "A High-Throughput Path Metric for Multi-Hop Wireless Routing," in Proc. of *ACM MobiCom 2003*, San Diego, California, Sep. 2003.

[4] R. Draves, J. Padhye and B. Zill, "Routing in Multi-Radio, Multi-Hop Wireless Mesh Networks," in Proc. of *ACM MobiCom 2004*, Philadelphia, Pennsylvania, USA, Sep. 2004.

[5] S. Lee, B. Bhattacharjee and S.Banerjee, "Efficient Geographic Routing in Multihop Wireless Networks," in Proc. of *ACM MobiHoc 2005*, Urbana-Champaign, Illinois, USA, May 2005.

[6] S. Rayanchu, A. Mishra, D. Agrawal, S. Saha and Su. Banerjee, "Diagnosing Wireless Packet Losses in 802.11: Separating Collision from Weak Signal," in Proc. of *IEEE INFOCOM 2008*, Phoenix Arizona, USA, Apr. 2008.

[7] C. Reis, R. Mahajan, M. Rodig, D. Wetherall and J. Zahorjan, "Measurement-Based Models of Delivery and Interference in Static Wireless Networks," in Proc. of *ACM SIGCOMM 2006*, Pisa, Italy, Sep. 2006.

[8] A. Kashyap, S. Ganguly and S. R. Das, "A Measurement-Based Approach to Modeling Link Capacity in 802.11-Based Wireless Networks," in Proc. of *ACM MobiCom 2007*, Montreal, Canada, Sep. 2007.

[9] L. Qiu, Y. Zhang, F. Wang, M. Han and R. Mahajan, "A General Model of Wireless Interference", in Proc. of *ACM MobiCom*, Montreal, Canada, Sep. 2007.

[10] Md. Rajibul Islam and Walaa Hamouda, "An efficient MAC protocol for cooperative diversity in mobile ad hoc networks," *Wireless Communications and Mobile Computing*, vol. 8, no. 6, pp. 771-782, Aug. 2008.

[11] Mohamed H. Ahmed, Halim Yanikomeroglu and Samy Mahmoud, "Interference management using base station coordination in broadband wireless access networks," *Wireless Communications and Mobile Computing*, vol. 6, no. 1, pp. 95-103, Feb. 2006.

[12] IEEE, "IEEE Standard for Wireless LAN-Medium Access Control and Physical Layer Specification," IEEE, 1990.

[13] IEEE, "IEEE Std. 802.11a-1999, Part 11: Wireless LAN Medium Access Control (MAC) and Physical Layer (PHY) specifications," IEEE Std. 802.11a, 1999.

[14] John G. Proakis, Digital Communications 4th Edition, McGRAW-HILL, 2001.

[15] Q. Chen, F. Schmidt-Eisenlohr, D. Jiang, M. Torrent-Moreno, L. Delgrossi and R. Morris, "Overhaul of IEEE 802.11 Modeling and Simulation in NS-2," in Proc. of *ACM MSWiM 2007*, Chania, Crete Island, Greece, Oct. 2007.

[16] X. Yang and H. Vaidya, "On the Physical Carrier Sense in Wireless Ad-hoc Networks," in Proc. of *IEEE INFOCOM 2005*, Miami, Florida, USA, Mar. 2005.

[17] H. Zhai and Y. Fang, "Physical Carrier Sensing and Spatial Reuse in Multirate and Multihop Wireless Ad-hoc Networks," in Proc. of *IEEE INFOCOM 2006*, Barocellona, Spain, USA, Apr. 2006.

[18] J. Lee, W. Kim, S. Lee, and Y. Choi, "An Experimental Study on the Capture Effect in 802.11a Networks," in Proc. of *ACM WiNTECH 2007*, Montreal, Canada, Sep. 2007.

Shinuk Woo received his B.S.E. degree in the School of Electrical Engineering at Korea University, Seoul, in 2007. He is currently an M.S.E student in the School of Electrical Engineering at Korea University. His research interests include ad-hoc routing, performance evaluation and analysis, and protocol optimization in wireless networks.

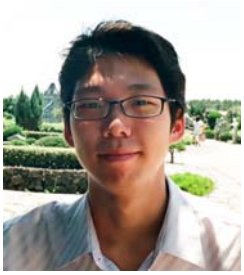

Jinpyo Hong received his B.S.E. degree in the School of Electrical Engineering at Korea University, Seoul, in 2008. He is currently an M.S.E student in the School of Electrical Engineering at Korea University. His research focuses on performance modeling and analysis in network systems, and practical security in community wireless networks.

Hwangnam Kim received his Ph.D. degree in Computer Science at the University of Illinois at Urbana-Champaign in 2004. He received his M.S.E. degree from the Department of Computer Engineering at Seoul National University, Seoul, Korea, in 1994, and received his B.S.E. degree from the Department of Computer Engineering at Pusan National University, Busan, Korea, in 1992. He is currently an associate professor in the School of Electrical Engineering at Korea University, Korea. He was a senior engineer at Samsung Electronics Co., Ltd., from 2005 to 2006, and had been a post-doctorate fellow in the Department of Computer Science at the University of Illinois at Urbana-Champaign, Illinois from 2004 to 2005. He had worked for Bytemobile Inc., California, from 2000 to 2001. He had worked for LG Electronics Ltd., Seoul, Korea, from 1994 to 1999. His research interests are in the areas of network modeling and simulations, wireless sensor networks, community wireless networks, pervasive/ubiquitous computing, and cyber physical systems.